AIP | The Journal of Chemical Physics

Multiscale reactive molecular dynamics

Chris Knight, Gerrick E. Lindberg, and Gregory A. Voth

Citation: The Journal of Chemical Physics **137**, 22A525 (2012); doi: 10.1063/1.4743958
View online: http://dx.doi.org/10.1063/1.4743958
View Table of Contents: http://scitation.aip.org/content/aip/journal/jcp/137/22?ver=pdfcov
Published by the AIP Publishing

Multiscale reactive molecular dynamics

Chris Knight,[1] Gerrick E. Lindberg,[2] and Gregory A. Voth[1,2,a)]
[1]*Computing, Environment, and Life Sciences, Argonne National Laboratory, Argonne, Illinois 60439, USA*
[2]*Department of Chemistry, James Franck Institute, Institute for Biophysical Dynamics, and Computation Institute, University of Chicago, Chicago, Illinois 60637, USA*

(Received 31 May 2012; accepted 25 July 2012; published online 15 August 2012)

Many processes important to chemistry, materials science, and biology cannot be described without considering electronic and nuclear-level dynamics and their coupling to slower, cooperative motions of the system. These inherently multiscale problems require computationally efficient and accurate methods to converge statistical properties. In this paper, a method is presented that uses data directly from condensed phase *ab initio* simulations to develop reactive molecular dynamics models that do not require predefined empirical functions. Instead, the interactions used in the reactive model are expressed as linear combinations of interpolating functions that are optimized by using a linear least-squares algorithm. One notable benefit of the procedure outlined here is the capability to minimize the number of parameters requiring nonlinear optimization. The method presented can be generally applied to multiscale problems and is demonstrated by generating reactive models for the hydrated excess proton and hydroxide ion based directly on condensed phase *ab initio* molecular dynamics simulations. The resulting models faithfully reproduce the water-ion structural properties and diffusion constants from the *ab initio* simulations. Additionally, the free energy profiles for proton transfer, which is sensitive to the structural diffusion of both ions in water, are reproduced. The high fidelity of these models to *ab initio* simulations will permit accurate modeling of general chemical reactions in condensed phase systems with computational efficiency orders of magnitudes greater than currently possible with *ab initio* simulation methods, thus facilitating a proper statistical sampling of the coupling to slow, large-scale motions of the system. © *2012 American Institute of Physics*. [http://dx.doi.org/10.1063/1.4743958]

I. INTRODUCTION

Many phenomena in condensed phase systems of interest to chemists, biologists, and material scientists involve chemical processes spanning multiple time and length scales. This situation introduces various challenges that need to be overcome if one is to simulate these systems with a sufficiently accurate model to capture the essential physics and properly sample the required system sizes and time scales in order to statistically converge the calculated properties of interest. Condensed phase simulation methods that explicitly treat electronic degrees of freedom,[1–5] which include the possibility for modeling chemical reactions, are naturally the first method of choice; but they come at a significant computational expense, thus limiting the accessible length and time scales. Also, current *ab initio* molecular dynamics (AIMD) simulations that are calculated by using density functional theory require validation from more accurate Schrödinger wavefunction methods. Empirical models that retain the accuracy and essential physics of electronic structure methods can instead be used to calculate molecular simulations at a greatly reduced computational cost, thus making them invaluable for modeling phenomena in heterogeneous condensed phase systems, which may contain several long length and timescale components and complex interfaces. The situation, however, requires more care when chemical reactions are involved; and an accurate determination of the reaction barriers in the condensed phase environment is necessary. The latter also requires a proper statistical sampling of slow degrees of freedom that may be coupled to the reaction of interest. The multistate empirical valence bond (MS-EVB) method[6,7] is one such empirical reactive MD method that has been exclusively used to model the complex process of proton solvation and transport.[8]

The accurate modeling of a condensed phase system is particularly challenging when multiple electronic excited states are involved as typical of nonadiabatic processes. The computational cost for the nonadiabatic *ab initio* simulation methods can be more expensive than ground-state methods, which further limits the applicable system sizes and times that can be simulated.[9–12] Highly accurate methods such as coupled-cluster algorithms[13] are sometimes required to properly describe excited states, but these methods are currently limited to small molecules, thus making any attempt at simulating nonadiabatic chemical reactions in condensed phase systems with the same method infeasible. Clearly, a sufficiently general algorithm is needed to develop reactive MD models (adiabatic or nonadiabatic) that are independent of the electronic structure method used for the reference calculations *and* that are able to account for variable bond topology to model chemical reactions. These models could then be used to address the challenges of converging statistical properties relating to multiscale reactive phenomena in complex,

a)Author to whom correspondence should be addressed. Electronic mail: gavoth@uchicago.edu.

condensed phase systems. The work described in this paper provides such a model.

Several MS-EVB models have been recently developed to model protonic defects.[14–19] Charge-ring models have successfully reproduced many structural properties of aqueous hydroxide,[16,20,21] but MS-EVB models with this architecture have been shown to suffer from large, currently undiagnosed, energy drifts.[16] Wick and Dang[15] and Wick[18] used experimental properties and *ab initio* calculations of clusters to parameterize MS-EVB models for hydroxide and hydronium. The hydronium model[18] results in a more localized excess proton ($c_1^2 = 0.896 \pm 0.002$) when compared to the previously reported occupation of MS-EVB states ($c_1^2 \approx 0.6$).[19] The increased localization of the excess proton will result in a reduced effective radius, which is expected to affect defect transport and affinity for the liquid-vapor interface. Some of these models,[15,18] including one for bulk water,[22] incorporate molecular polarization via configuration dependent electrostatics (e.g., bond distance-dependent atomic charges and/or induced point polarizabilities), in addition to the delocalization of the proton defect across multiple molecules in MS-EVB, which may lead to an unphysical overestimation of polarization. To our knowledge there have been no extensive studies of the charge distribution of molecular models containing both configuration dependent electrostatics in multistate reactive models, but AIMD simulations and nonreactive polarizable simulations have been shown to result in distinctly different induced dipole distributions.[23] Instead of parameterizing models based on gas-phase clusters, this work aims to exclusively employ information from condensed phase *ab initio* simulations to systematically force match reactive models based on results in a self-consistent forcefield faithful to the reference *ab initio* simulation.

In our previous work, a force-matching (FM) algorithm was developed that used data directly from a condensed phase *ab initio* simulation to determine effective interactions between nuclei for an empirical reactive MS-EVB model of the hydrated excess proton.[24] The FM method was sufficiently flexible that those interactions expected to dominate far from the reactive species could be defined by using previously parameterized empirical models for those regions (e.g., pure solvent or protein forcefield). Those portions of the model describing interactions with and between the reactive species could then be separately fit by using data from AIMD simulations. However, in that earlier work the functional forms for the interactions in the reactive MD model were chosen to be the same predefined empirical functions that had been used in an earlier MS-EVB model for the excess proton.[19] The algorithm presented here, on the other hand, provides a significant advantage by enabling the linear least-squares optimization of tabulated expressions, thereby removing any possible artifacts introduced by empirical functions that may constrain the accuracy of the resulting FM model. Linear FM methods also have the advantage of no longer requiring the nonlinear optimizations of several parameters, which may be slow to converge or plagued with multiple, possibly unphysical, local minima. The present model can therefore be considered to be "multiscale" in that it connects electronic structure to effective reactive forces between the nuclei, but it is no longer "empirical" in the sense that predefined empirical analytical functions are not used to represent those effective forces.

The procedure used to develop these new reactive MD models is actually a generalization of the multiscale coarse-graining (MS-CG) method.[25–29] The MS-CG method reduces the complexity of the original system by constructing a reduced coarse-grained system with significantly fewer degrees of freedom, the dynamics of which are governed by a set of effective interactions. For AIMD simulations, the original nuclear+electron system can thus be mapped to a reduced representation containing only nuclei.[21] With the electronic degrees of freedom integrated away, a set of effective interactions between nuclei, determined by using a variational force-matching algorithm, can be used to sample the long-time motion of the nuclear degrees of freedom at a significantly reduced computational cost. The elimination of the electronic degrees of freedom is analogous to the development of "solvent-free" coarse-grained models in which the solvent degrees of freedom are integrated away.[30,31] The resulting effective interactions are obtained by averaging over the electronic wavefunction distribution similar to the case of averaging over solvent configurations. Although the nuclear degrees of freedom have not been coarse-grained, the integration over the electronic degrees of freedom leaves an effective, "coarse-grained" interaction between nuclei. With the proper modification, the MS-CG methodology is sufficiently general and provides a systematic procedure that can be used to efficiently parameterize both nonreactive and reactive MD models, such as the framework used in this work, that account for the dynamic formation and breaking of chemical bonds.

In this work, a new iterative FM algorithm is developed that enables one to construct reactive models using flexible, tabulated interactions as opposed to empirical functions. The resulting models enable multiscale reactive molecular dynamics (MS-RMD) models for chemical reactions in condensed phase systems using a set of accurate interaction potentials. The MS-RMD method has the additional benefit of using a linear least-squares method to determine model parameters, which eliminates the complexities associated with the nonlinear optimizations of empirical functions.

Section II will first summarize the AIMD method used to generate configurational distributions used as input to the FM-based MS-RMD algorithm. The core reactive MD methodology is then briefly reviewed. Next, attention turns to nonreactive models for both the hydronium cation and hydroxide ion, which serve as the foundation for the corresponding MS-RMD models. The iterative FM algorithm then is presented and used to generate reactive models for both charged-defects. Section III discusses the favorable agreement of results from the FM MS-RMD models with those from the original AIMD simulations. Section IV summarizes the work and its potential benefits.

II. METHODS AND DEVELOPMENT

A. Condensed phase *ab initio* MD simulations

The configurations used as input to the force-matching algorithms discussed in this work were generated from

Born-Oppenheimer molecular dynamics simulations calculated by using the Quickstep module in the CP2K software package.[1] The Becke-Lee-Yang-Parr (BLYP) (Refs. 32 and 33) density functional was used with empirical dispersion corrections[34] for all AIMD simulations. The use of dispersion-corrected density functionals lead to improved properties of water at ambient conditions, such as the equilibrium density and an increase in the water self-diffusion constant for the BLYP functional.[35–39] The equations of motion for the nuclei were integrated with a 0.5 fs timestep, and the electronic orbitals were optimized to the Born-Oppenheimer surface by using an orbital transformation method[40] with a convergence criterion of 10^{-7}. The wavefunction was expanded in the Gaussian TZV2P basis set, the auxiliary electron density was expanded in plane waves up to 400 Ry, and Goedecker-Teter-Hutter pseudopotentials[41] were used. The initial configurations for both the excess proton and hydroxide simulations were generated by adding and removing a proton, respectively, from a previously equilibrated bulk water simulation containing 128 water molecules with a lattice constant of 15.66 Å. The newly created systems were each equilibrated in the constant *NVT* ensemble for 25 ps and then continued in the *NVE* ensemble for an additional 72 and 76 ps for the proton and hydroxide systems, respectively. The AIMD simulation for the hydroxide ion discussed here is the same one used recently to develop nonreactive two-site and charged-ring models for the hydroxide ion.[21] In addition, two extra 32 ps constant *NVE* simulations were completed for each charged defect in order to calculate dynamic properties and to reduce any bias of results due to initial conditions. The initial configurations for these additional simulations were selected from simulations calculated with the corresponding FM nonreactive models and equilibrated in the constant *NVT* ensemble for 5 ps. The average temperature of all constant *NVE* simulations was 306.8 ± 1.4 and 301.6 ± 4.1 K for the excess proton and hydroxide systems, respectively.

B. Reactive MD

The modeling of chemical reactions requires a methodology that can dynamically alter the bonding topology of the system over the course of a simulation in response to changes in the environment and the intrinsic quantum mechanics of the reaction. *Ab initio* methods that explicitly treat the electronic degrees of freedom are a natural choice for a methodology, but they come at a significant computational expense. One set of solutions to address this challenge that remain feasible even for large-scale condensed phase systems are multistate[6,7,21,42–48] and multiconfigurational[49,50] molecular mechanics methods. In brief, multistate methods treat the system as a linear combination of several possible bonding topologies (diabatic states) that are coupled to one another through the off-diagonal elements of a quantum-like Hamiltonian matrix. In particular, the MS-EVB algorithm is a generalization of the original EVB (Refs. 43 and 44) approach that adapts and dynamically identifies bonding topologies to include as the simulation progresses. These bonding topologies form a basis of diabatic states that are used to evaluate elements of the Hamiltonian matrix. The subset of molecules described with variable bonding topology at any point in time during a simulation form the reactive complex. Examples of reactive complexes are shown in Fig. 1 for both the excess proton and hydroxide. The diagonal entries, V_{jj}, of this effective Hamiltonian typically are evaluated by using molecular mechanics forcefields, V_{MM}, with additional diabatic corrections, V_{CORR}, that tend to be repulsive. The off-diagonal couplings, V_{jk}, provide the mechanism for the system to transition between bonding topologies, and therefore to describe chemical reactions. Typical empirical definitions for the off-diagonal couplings are simple geometric functions, A_{GEO}, of the donor-acceptor distance, such as Gaussian, hyperbolic tangent functions, distributed Gaussians,[51] or spline fits,[18] to reproduce potential energy surfaces calculated from gas-phase clusters. Recently, genetic programs have also been used to explore both function and parameter space for defining interactions in MS-EVB models.[52] In order to go beyond just the local geometry, electrostatic interactions, V_{EX}, must be included in the condensed phase to account for effects due to the environments that may alter the stability of configurations near a transition state. The specific effective Hamiltonian terms are given by

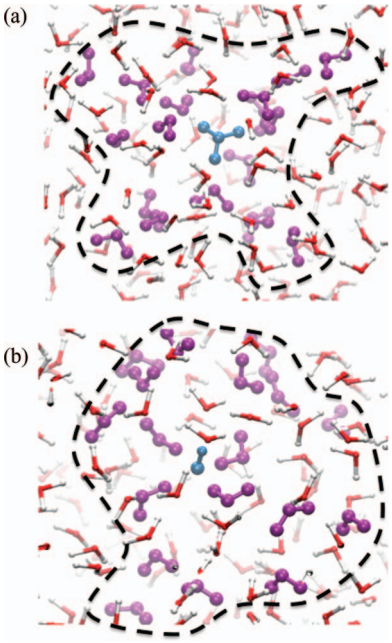

FIG. 1. Example of the reactive complexes formed for the (a) excess proton and (b) hydroxide ion. The dashed line indicates the boundary between those atoms within the reactive complex and the rest of the system, which dynamically changes over the course of a simulation.

$$V_{jj} = V_{MM} + V_{CORR}, \tag{1}$$

$$V_{jk} = (V_{CONST} + V_{EX})A_{GEO}. \tag{2}$$

When electrostatic interactions are included in the off-diagonal, a constant, V_{CONST}, that would normally be absorbed into the geometric factor as a prefactor is kept separate in order to shift the zero of the electrostatic energy.[19,42,47,48] In this case, the electrostatic energy modulates the prefactor

of the original geometric factor. The diabatic correction term, V_{CORR}, used here was labeled in previous MS-EVB models as a repulsive interaction, V_{REP}.[19,24,42,47,48] This term is labeled now as a general correction because no constraints on the functional form are enforced in the FM algorithm presented here and it is thus possible that this interaction could be attractive if the underlying molecular mechanics forcefield had too large of an energetic penalty for sampling regions of phase space near a reactive transition state. With the FM algorithm presented here, the diabatic corrections and off-diagonal geometric factor can be expressed as general, flexible, tabulated potentials as opposed to a set of empirical functions that may or may not have been validated. As such, these functions bridge in a multiscale fashion the MS-RMD model to the real quantum Hellman-Feynman forces via force-matching into actual, as opposed to empirical, effective interactions. In the absence of empirical functions, the interactions in the resulting MS-RMD models can be used to justify the choice of empirical functions used in previous work.

C. Force-matching nonreactive models

1. Hydronium ion

The models used in MS-RMD simulations are based in part on a molecular mechanics forcefield, which serves as the major contribution to the diagonal elements of the Hamiltonian matrix (we note that this is not in principle necessary but it is convenient). As in previous work, the reactive models developed here were constructed in stages: first the nonreactive model was developed, and then the reactive model was constructed. The Hellman-Feynman theorem (HFT) forces from the *ab initio* Born-Oppenheimer simulations of the excess proton were used as input for a FM algorithm, where a residual, Eq. (3), measuring the ensemble average of the squared difference in the AIMD HFT forces and effective forces was minimized[21]

$$\chi^2 = \frac{1}{3N}\left\langle \sum_{j=1}^{N} \left|\mathbf{F}_j^{\mathrm{HFT}} - \mathbf{F}_j^{\mathrm{EFF}}\right|^2 \right\rangle. \quad (3)$$

The nonreactive model for the hydronium cation was parameterized following the same procedure used to previously derive a model from a condensed phase AIMD simulation using the Hamprecht-Cohen-Tozer-Handy (HCTH) density functional.[24] The intramolecular model for the hydronium cation was the same as previously used, and the SPC/Fw water model[53] was used as opposed to fitting a new water model based on the AIMD simulation results. With the intramolecular and electrostatic parts of the model defined, the remaining nonbonded interactions between the hydronium cation and water molecules were determined by force-matching to the HFT forces obtained from AIMD simulations. In order to accomplish this, a subset of configurations from the AIMD trajectory was selected for the FM procedure, such that the solvation structure of the hydronium cation closely resembled the Eigen cation, $H_9O_4^+$, the resting state of the charged excess proton defect.[54,55] The criterion for selecting these configurations was based on the smallest value of a proton transfer order parameter, $\delta > 0.2$ Å, calculated as the difference between the H-bond and covalent bond distances for a specific H-bonded hydronium-water pair.[24,55]

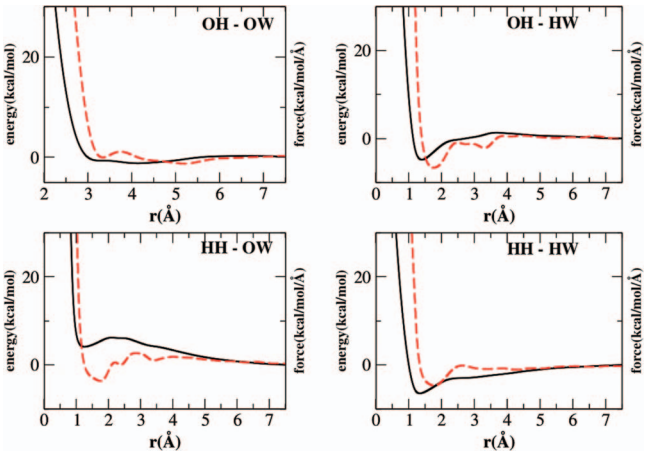

FIG. 2. Pairwise potentials (solid lines) and forces (dashed lines) from the B-spline fits for hydronium-water interactions plotted as a function of interatomic separation. The atom labels are defined in the text.

The interatomic pairwise potentials to be fit were defined to be a linear combination of interpolating functions (cubic splines). The contributions to the CG forces that were already defined (intramolecular, electrostatic, SPC/Fw) were first subtracted from the HFT forces, and the atomic force residual was used in the minimization of Eq. (3). Each interatomic pairwise potential was represented on a grid with a spacing of 0.1 Å. The tabulated force and its first two derivatives were constrained to be zero at the cutoff distance of 7.8 Å. The coefficients for these spline functions were determined as the linear least-squares minimization of the residual in Eq. (3) by solving an overdetermined system of equations.[56–58] At the shortest distances for each interatomic pair, where the sampling is limited, the forces were extrapolated to shorter distances by using a fit of $1/r^n$, where the exponent n was chosen based on smoothness. These extrapolated force curves were then fit to B-splines in order to eliminate statistical noise in the force curves and improve energy conservation. The B-spline fitted force curves for the hydronium-water interactions are shown in Fig. 2, and the coefficients are listed in Table I. The atom types used in Fig. 2 and elsewhere are labeled as two characters, with the first letter defining the element and the second letter defining the molecule. For example, "OH" denotes the oxygen of hydronium (or hydroxide depending on the model) and "HW" corresponds to the hydrogen atom of a water molecule.

2. Hydroxide ion

The nonreactive hydroxide model developed here is based on the two-site model from a previous study[21] with an additional three-body interaction included. Hydroxide ions commonly are over-coordinated in bulk water when using simple two-site models, and thus more complicated models are required using, for example, three-body potentials or a charge-ring model.[15,16,20,21] With the two-site hydroxide model[21] as a starting point, a three-body interaction involving the hydroxide bond and proximal water oxygen atoms

TABLE I. B-spline coefficients for each hydronium-water interatomic pair in the nonreactive model. The values of r_{core} used in the B-spline fits are 2.0, 1.2, 0.9, and 1.2 Å for the OH–OW, OH–HW, HH–OW, and HH–HW interatomic pairs, respectively. The evenly spaced bin widths for the corresponding curves were 0.58, 0.33, 0.23, and 0.33 Å. The value of r_{cut} remained at 7.8 Å and a polynomial order of 6 was used for all curves. Trailing zeroed coefficients for each curve are omitted for clarity, and the resulting curves are shown in Fig. 2.

n	OH–OW	OH–HW	HH–OW	HH—HW
1	142.3787	30.6048	158.1527	13.1760
2	119.7021	12.8241	76.6490	3.7248
3	74.9776	− 1.3372	16.3827	− 3.5881
4	45.3455	− 7.5645	1.4867	− 3.4542
5	− 20.9843	− 5.9280	− 2.2173	− 6.0079
6	11.2329	− 9.0470	− 2.7144	− 4.3451
7	− 3.9884	3.6121	− 3.5742	0.1435
8	1.5298	− 4.5015	− 5.2106	0.2671
9	− 3.3958	2.1488	5.0724	− 1.1518
10	1.0618	− 6.2932	− 4.0822	− 0.8201
11	− 1.1024	3.1139	4.5130	− 1.0234
12	0.9083	− 0.8365	1.5914	− 0.3816
13	− 0.4423	1.2911	3.8124	− 1.8704
14	0.8274	0.4376	− 0.1383	− 0.0519
15	− 0.3076	0.3791	1.5763	− 1.4096
16	0.1095	0.0871	1.5115	− 0.3603
17		− 0.0013	2.1562	− 0.5254
18		0.7607	1.5052	− 0.2139
19		− 0.3421	1.8256	− 0.3881
20		1.2020	1.4905	− 0.4447
21		− 0.0946	1.2609	− 0.3272
22		0.1670	1.1820	− 0.0429
23		− 0.2593	1.0116	− 0.4616
24		0.1893	0.6997	− 0.1153
25		− 0.0451	1.0547	− 0.0973
26		0.0228	0.5954	0.0153
27			0.4978	
28			0.7561	
29			0.6394	
30			0.2425	
31			0.3365	
32			0.3206	
33			0.3029	
34			0.1039	
35			0.0483	
36			− 0.0025	

(HH–OH–OW) was included in the model. The optimal parameters for a Stillinger-Weber (SW) potential,[59] Eq. (4), were determined by using a Simplex algorithm and fitting the residual force difference, Eq. (3), defined between the original two-site hydroxide model and the AIMD simulation results. The form of the SW potential used is given by

$$V_{\mathrm{SW}}(r_1, r_2, \theta) = \varepsilon(cos\theta - cos\theta_0)^2 \exp\left(\frac{\sigma}{r_1 - \sigma}\right)\exp\left(\frac{\sigma}{r_2 - \sigma}\right). \tag{4}$$

The optimized values of the parameters are $\varepsilon = 271.6$ kcal/mol, $\theta = -0.290$ rad, and $\sigma = 4.0$ Å. As discussed below, the addition of this three-body potential to the nonreactive model produces a considerable improvement in the hydroxide ion solvation structure, as observed in the hydroxide-water angle distribution (HH–OH–OW).

D. Force-matching reactive models

1. Iterative FM algorithm

A straightforward application of a linear least-squares method for the parameterization of a MS-RMD model is complicated by the fact that the forces are known only after the multistate Hamiltonian has been constructed and diagonalized and the Hellman-Feynman theorem used with the coefficients of the ground-state eigenvector, such that

$$\mathbf{F}_j^{\mathrm{HFT}} = -\langle\Psi_0|\frac{\partial \mathbf{H}}{\partial \mathbf{r}_j}|\Psi_0\rangle = \sum_{m,n} c_m c_n \mathbf{F}_j^{mn}. \tag{5}$$

If the coefficients for the MS-RMD ground state for an ensemble of configurations were known *a priori*, then it would be straightforward to express each component of the force, $\mathbf{F}_j^{mn}$, as a linear combination of interpolating functions (cubic splines), and the resulting total atomic force, $\mathbf{F}_j$, would be a linear function of the model parameters to be determined. However, this is not the case. Another possible issue is the nonlinear dependencies introduced in the definition of the MS-RMD model, such as the off-diagonal couplings being defined as an electrostatic energy multiplied by a local geometric factor, Eq. (2). If the geometric factor, A_{GEO}, was defined to be a linear function of model parameters, then the nonlinearity introduced by multiplication with the electrostatic energy and constant could be handled by using two separate optimizations: linear and nonlinear. With an initial guess for the nonlinear parameters, a linear least-squares optimization could be used to determine those parts of the model that depend linearly on model parameters, such as A_{GEO}. After the linear optimization completes, the nonlinear parameters could be optimized holding the new set of linear parameters fixed. Afterwards, the linear portion of the model could be reoptimized by using the new set of nonlinear parameters and the procedure repeated until converged. By defining a large fraction of the model as being linear with respect to the model parameters, the cost of the nonlinear optimization can be significantly reduced by requiring the optimization of only a few parameters.

If one chooses to use this type of iterative algorithm to reduce the cost of the parameter optimization due to nonlinearities in the model, then an immediate solution to the problem of not knowing the ground state MS-RMD coefficients *a priori* is to provide an initial guess and then include the convergence of the eigenvector as part of the criteria for reaching self-consistency. This is the main motivation behind the FM algorithm outlined in Fig. 3 for a single set of values for the nonlinear parameters. In this algorithm, an initial Hamiltonian matrix is constructed by using educated guesses for all model parameters, the Hamiltonian matrix is diagonalized, and the coefficients of the ground state eigenvector determined. With this set of eigenvector coefficients and fixed values for the nonlinear parameters, the atomic forces in Eq. (5), which are linear functions of the remaining parameters, are variationally optimized by using a linear least-squares method to minimize

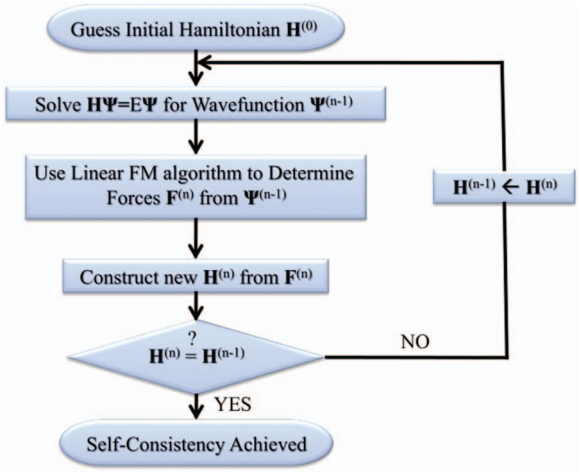

FIG. 3. Flow chart outlining the iterative force-matching algorithm used to develop reactive models.

the residual in Eq. (3). With the new set of linear parameters, a new guess for the Hamiltonian matrix can be constructed and diagonalized in order to update the coefficients of the ground state eigenvector to be used to calculate a new set of linear parameters. This procedure is iterated until self-consistency has been reached for the ground state eigenvector and linear model parameters. This algorithm for defining the MS-RMD interactions, V_{CORR} and A_{GEO}, as linear combination of interpolating functions was found to converge in three to five iterations for both the proton and hydroxide ion models using forces calculated from an AIMD condensed phase simulation. If there were nonlinear parameters in the model to be determined, they would be optimized by using an algorithm such as Simplex with the other portions of the model fixed, including the linear parameters, identical to the procedure used in previous work.[24] With the current algorithm, however, the number of nonlinear parameters has been significantly reduced. The procedure described here for separately optimizing the linear and nonlinear parameters can then be repeated sequentially until both sets of parameters have converged to their optimal values.

The main advantages of this algorithm are the ability to define interactions as flexible tabulated expressions and the reduction in computational cost associated with a nonlinear optimization. For the reactive models developed here, the remaining nonlinear parameters are contained in the definition of the off-diagonal coupling as the prefactor to the geometric factor. The off-diagonal constant and exchange charges are the only four parameters that need to be determined by using a nonlinear optimization algorithm. The diabatic corrections and local geometric factor are described by using spline functions, the same definition used for the pairwise interactions of the nonreactive hydronium and hydroxide models.

2. Excess proton

For the reactive model describing the hydrated proton, the initial guess for the four nonlinear parameters was taken from a previously developed model derived from condensed phase simulations with the HCTH density functional.[24] Similar to the MS-EVB3 model for the excess proton, two diabatic corrections were defined as part of the model developed here: one for the hydronium-oxygen and water-oxygen atoms, V_{REP}^{OO}, and one between hydronium-hydrogen and water-oxygen atoms, V_{REP}^{HO}, such that

$$V_{CORR} = V_{REP}^{OO} + V_{REP}^{HO}. \quad (6)$$

The off-diagonal geometric factor, A_{GEO}, was defined to be a function of the distance between the hydronium-oxygen and water-oxygen involved in the H-bond of the transferring proton. The forces for each of these three pairwise functions were represented on a grid with a spacing of 0.1 Å. The tabulated force and its first two derivatives were constrained to be zero at the cutoff distance of 2.9, 1.3, and 3.2 Å for the V_{REP}^{OO}, V_{REP}^{HO}, and A_{GEO} interactions, respectively. For the initial iteration, the diabatic corrections were set to zero, and the off-diagonal geometric factor was set to one for all donor-acceptor distances. With the iterative algorithm outlined in Fig. 3, the coefficients for these spline functions were determined as the linear least-squares optimization of the residual in Eq. (3) by solving an overdetermined system of equations.[56–58] At the shortest distances for each pairwise function, the forces were extrapolated to shorter distances by using a linear fit. These extrapolated force curves were then fit to B-splines to eliminate statistical noise in the force curves and improve energy conservation. The B-spline fitted curves were used for each step of the iterative FM algorithm in Fig. 3. The B-spline fitted force curves for the reactive proton model are shown in Fig. 4, and the polynomial coefficients are listed in Table II. In the final set of four nonlinear parameters, the off-diagonal exchange charges were found to be similar to the initial values used at the start of the fitting process. Based on this result, the iterative FM algorithm was repeated with the off-diagonal exchange charges fixed at the values from

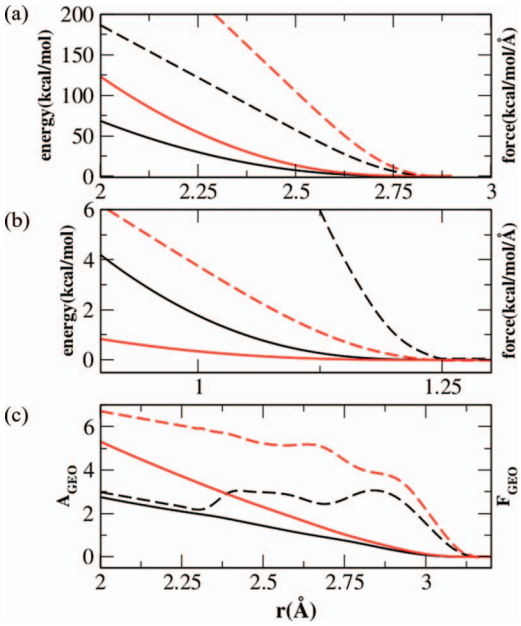

FIG. 4. Tabulated potentials (solid lines) and forces (dashed) for diabatic corrections (a) V_{REP}^{OO}, (b) V_{REP}^{HO} in Eq. (6) and off-diagonal geometric factor (c) A_{GEO} in Eq. (2) for the excess proton (black) and hydroxide ion (red) reactive models.

TABLE II. B-spline coefficients for the diabatic corrections and off-diagonal geometric factor for the reactive excess proton model. The values of r_{core} used in the B-spline fits are 2.0, 0.8, and 2.1 Å for the V_{REP}^{OO}, V_{REP}^{HO}, and A_{GEO} interactions, respectively. The evenly spaced bin widths for the corresponding curves were 0.085, 0.045, and 0.0525 Å. The value of r_{cut} was 2.85, 1.25, and 3.15 Å for the corresponding curves, and a polynomial order of 6 was used for all curves. Trailing zeroed coefficients for each curve are omitted for clarity, and the resulting curves are shown in Fig. 4.

n	V_{REP}^{OO}	V_{REP}^{HO}	A_{GEO}
1	186.8016	41.2160	2.7165
2	183.1398	40.3683	2.7125
3	175.7715	38.6700	2.6192
4	164.7942	36.1281	2.6283
5	150.0428	32.7296	2.4218
6	131.7579	28.4960	2.4187
7	109.6329	23.3915	2.2148
8	87.7021	18.3660	1.8722
9	65.5203	13.3516	3.3914
10	43.7042	8.7389	2.9196
11	23.6742	4.6277	3.0227
12	10.3514	2.1909	2.9306
13	3.8574	0.5109	2.8816
14	1.0625	0.3833	2.4445
15	0.4695	0.0700	2.3205
16	0.1798	0.0486	2.6821
17			3.1176
18			3.1232
19			2.8403
20			2.0784
21			1.2542
22			0.5621
23			0.2077
24			0.0695
25			0.0269
26			0.0069

the previous model, leaving only the off-diagonal constant as a parameter to be optimized by using a simple line search. The values for the nonlinear parameters for the reactive proton model are listed in Table III.

3. Hydroxide ion

The development of a reactive model for the hydroxide ion followed the same procedure as discussed in Sec. II D 2 for the excess proton. The definition of this model included similar definitions for the diabatic corrections and off-diagonal geometric factor as pairwise functions between the hydroxide-oxygen and water molecule atoms. The initial values for the four nonlinear parameters were again taken from the previous excess proton model,[24] as opposed to selecting a random set of initial values. The details of fitting the three tabulated potentials to spline functions were the same as for the reactive proton model developed in Sec. II C. Although the use of an HH–OH–OW three-body correction was found to improve the solvation structure of the nonreactive two-site hydroxide model, initial tests with reactive models developed with this correction were found to yield long hydroxide lifetimes and thus a low rate of successful proton transfer events. Motivated by the three-body interaction used in a recently developed reactive model for the hydroxide ion,[15] a three-body interaction was defined to act between the hydroxide oxygen and two neighboring water oxygens (OW–OH–OW) using as a basis the same parameters as for the nonreactive HH–OH–OW interaction. While the OW–OH–OW interaction was not sufficient to reduce the degree of over-coordination observed in the underlying nonreactive two-site model, initial tests with reactive models were promising and thus this was the interaction form used to develop the model presented here. If one wanted to choose a more flexible basis, then additional three-body corrections could be force-matched using AIMD data, such as the coordination-dependent (3, 4, and 5 solvating water molecules) OW–OH–OW interaction used in a recent MS-EVB model for the hydroxide ion.[15]

TABLE III. Optimized model parameters for the off-diagonal couplings for FM reactive proton and hydroxide models.

	Excess proton	Hydroxide
V_{const}^{ij}(kcal/mol)	− 13.88	− 13.78
q_O^{ex}(e)	− 0.0500	− 0.0510
q_H^{ex}(e)	0.0167	0.0247
q_{H*}^{ex}(e)	0.0332	0.0526

Results from an initial reactive hydroxide model showed an increased population of the 5-coordinated solvation structure, with a peak in the hydroxide-water angle (HH–OH–OW) probability distribution near 180°, which was originally observed in the nonreactive model before introduction of the three-body potential. With the current definition for the local geometric factor, which depends only on the donor-acceptor distance, there is no distinguishing between water molecules in the square planar arrangement around the hydroxide ion or a water molecule that approached the hydroxide ion from below. Since transfer of a proton from a water molecule that approaches below the hydroxide ion was not observed in the AIMD simulations, the off-diagonal geometric factor was multiplied with an additional function that depends on the HH–OH–OW angle. This function was chosen to reduce the off-diagonal coupling when a water molecule donates an H-bond at an HH–OH–OW angle near 180°, while leaving the coupling for all other water molecules unchanged,

$$f(\theta) = \frac{1}{2}\left(1 - \tanh\left[\alpha\left(\theta - \theta_0\right)\right]\right). \tag{7}$$

The values of the parameters were chosen to be $\alpha = 0.25^{\circ -1}$ and $\theta_0 = 140^{\circ}$ based on the HH–OH–OW angle distribution as calculated from the AIMD simulations, Fig. 5. This neglect of certain diabatic states could have also been implemented as part of the state search algorithm, where an angle criterion would be used to determine which states are included in the diabatic basis used to construct the Hamiltonian matrix, but that would have likely resulted in states with significant coupling abruptly being included or removed from the Hamiltonian, leading to an increase in the drift of the total

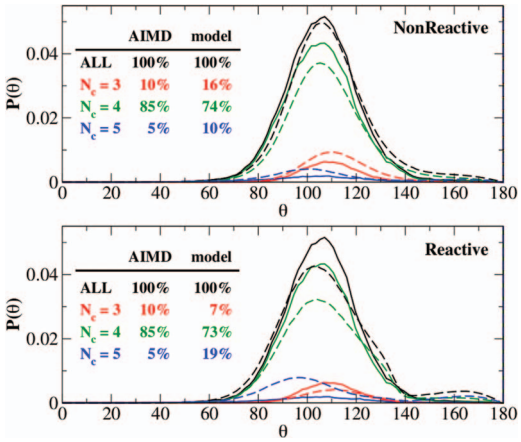

FIG. 5. Probability distributions for the hydroxide water-oxygen angle (HH–OH–OW) for the AIMD simulation (solid lines) and FM-based MS-RMD models (dashed lines). The full distribution (black) is decomposed into contributions from solvation structures with three (red), four (green), and five (blue) water molecules donating H-bonds to the hydroxide ion, with relative populations indicated.

energy. By using a smooth function of the system coordinates, the contribution from those states where a water molecule is donating an H-bond from below the hydroxide ion can be made negligible in a continuous manner. With the parameters for the angle-dependent function fixed, the iterative FM procedure was repeated in order to parameterize a reactive model for the hydroxide ion. The optimized nonlinear parameters are listed in Table III, the coefficients for the tabulated potentials are listed in Table IV, and the tabulated potentials are shown in Fig. 4.

TABLE IV. B-spline coefficients for the diabatic corrections and off-diagonal geometric factor for the reactive hydroxide model. The values of r_{core} used in the B-spline fits are 2.0, 0.9, and 2.3 Å for V_{REP}^{OO}, V_{REP}^{HO}, and A_{GEO} interactions, respectively. The evenly spaced bin widths for the corresponding curves were 0.085, 0.035, and 0.085 Å. The value of r_{cut} was 2.85, 1.25, and 3.15 Å for the corresponding curves and a polynomial order of 6 was used for all curves. Trailing zeroed coefficients for each curve are omitted for clarity and the resulting curves are shown in Fig. 4.

n	V_{REP}^{OO}	V_{REP}^{HO}	A_{GEO}
1	333.9791	6.1891	5.9091
2	327.4629	6.0462	5.9784
3	314.5365	5.7586	5.6280
4	294.9678	5.3307	5.9403
5	269.1527	4.7566	5.2448
6	236.5075	4.0525	5.2644
7	197.7903	3.2104	4.8854
8	158.5645	2.4098	5.7094
9	120.0611	1.6668	3.8874
10	80.2545	1.0334	3.7608
11	43.4640	0.5137	4.0839
12	18.4555	0.2308	1.7564
13	6.8357	0.0921	0.9765
14	1.8423	0.0046	0.0154
15	0.7601	− 0.0074	0.1343
16	0.2668	− 0.0229	− 0.0106

III. RESULTS AND DISCUSSION

A. Force-matched reactive models

The tabulated potentials for the diabatic corrections and off-diagonal geometric factor are shown in Fig. 4 and found to take similar shapes for both reactive proton and hydroxide models. The diabatic corrections take a relatively simple shape and are repulsive for all distances sampled. This result is in agreement with previous MS-EVB models that have defined these corrections as repulsive interactions modeled by using an exponential function.[16,19,42,47,48] For the off-diagonal geometric factors, however, there is structure in the forces, F_{GEO}, as a function of the donor-acceptor distance for an H-bond that the proton is transferring across, but the corresponding geometric factors are relatively featureless when viewed at the scale in Fig. 4. These peaks in the derivatives of the geometric factor would be missed with simple Gaussian or hyperbolic tangent functions typically used in EVB models. The functional form for the geometric factor used in the MS-EVB models for the excess proton,[19,42,47,48] which requires the optimization of seven parameters, would also have difficulty capturing the structure observed in the range of sampled distances 2.25–3.2 Å.

The force-matched reactive models developed in this work were used to generate independent trajectories in the constant *NVE* ensemble by using a modified version of the LAMMPS MD code.[60] The equations of motion for all simulations with FM models (nonreactive and reactive) were integrated by using a timestep of 0.5 fs unless otherwise stated. The state search algorithm developed for the MS-EVB3 model was used here with generalizations to model the transport of both the excess proton and hydroxide ion.[19]

The total energy drift for the nonreactive FM models was 0.16 ± 0.24 and 0.26 ± 0.13 kcal/mol per nanosecond for the hydronium and hydroxide models, respectively, as estimated from six 2.5 ns simulations each. The energy drifts relative to the total energy were 9.2×10^{-5} and 1.3×10^{-4} 1/ns for the nonreactive hydronium and hydroxide models. The total energy drift for the reactive proton model was 3.3 ± 3.8 kcal/mol per ns (2.1×10^{-3} 1/ns), as estimated from sixteen 400 ps simulations using a timestep of 0.50 fs. The drift in the total energy for the hydroxide reactive model was 5.8 ± 4.8 kcal/mol per ns (3.4×10^{-3} 1/ns), as estimated from twenty-two 300 ps simulations using a timestep of 0.5 fs. With a smaller timestep of 0.25 fs, the drift for the hydroxide model was reduced to 3.0 ± 3.8 kcal/mol per ns (1.8×10^{-3} 1/ns). The results of simulations for both reactive models are discussed below.

B. Excess proton

The hydronium-water radial distribution functions (RDFs) for the AIMD, nonreactive, and reactive models are shown in Fig. 6. Comparison of the four RDFs shows a general agreement with the AIMD data for both models in terms of the peak heights, positions, and integrated coordination numbers. One noticeable deviation is in the RDF for the hydronium-oxygen water-oxygen (OH–OW) interatomic pair with an enhanced peak at separations just larger than 3.0 Å.

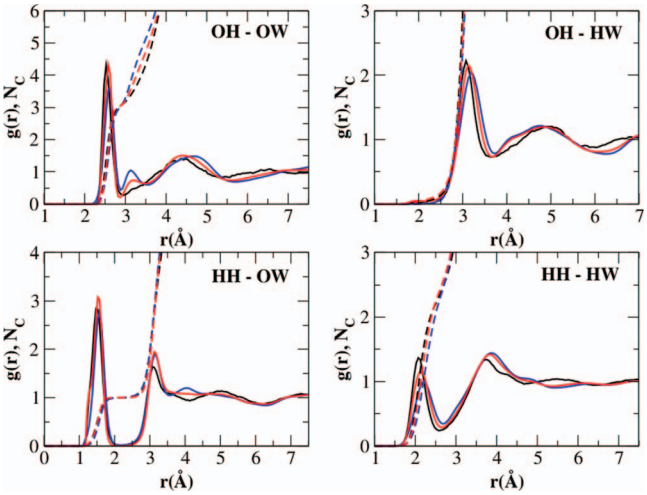

FIG. 6. Radial distribution functions (solid lines) and integrated coordination numbers (dashed lines) between atoms of the hydronium cation and water molecules. For each plot, results from the AIMD (black), nonreactive (blue), and reactive MS-RMD (red) models are shown. The atom labels are defined in the text.

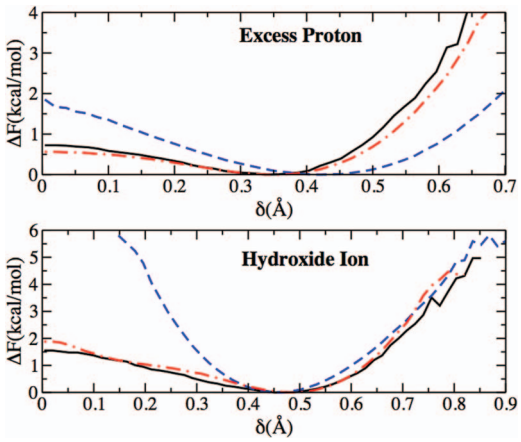

FIG. 7. Potentials of mean force along a proton transfer coordinate for the excess proton and hydroxide models. Results are shown for the AIMD (solid black), nonreactive (dashed blue), and reactive (dot-dashed red) models.

The density contributing to this peak principally comes from the second solvation shell peak (near 4.5 Å), where a water molecule that transitions in and out of the first solvation shell and which would be expected to weakly donate an H-bond to the lone pair side of the hydronium cation is bound too strongly. As discussed below for the hydroxide ion, it seems to be a general trend in these reactive models for charged defects that special attention needs to be focused on correctly describing relatively weak interactions compared with the strong H-bonds formed in the first solvation shell. The inclusion of a second set of pairwise potentials that are zero beyond the first solvation shell may assist in accurately capturing features in the solvation structure due to weaker H-bonds. There are some deviations in the RDFs beyond the second solvation shell, but this can be expected because the forces in that region are dominated by water-water interactions and the SPC/Fw water model used differs from the corresponding AIMD water model.

An important thermodynamic property for the transport of charged defects via the Grotthuss mechanism is the free energy barrier for proton transport. The proton transfer barrier calculated from the AIMD simulation is 0.72 kcal/mol for the CP2K simulation, Fig. 7, which is larger than the barriers of $\sim$0.6 and 0.5 kcal/mol calculated for the BLYP and HCTH density functionals, respectively.[24,61] The barrier height for the FM reactive model is 0.08 kcal/mol smaller than the AIMD result. The increased barrier height for proton transport with respect to the other density functionals is consistent with a corresponding reduction in the diffusion constant of the excess proton. The diffusion constant for the excess proton calculated from the current AIMD simulations is 0.44 ± 0.33 Å^2/ps to be compared with the diffusion constants of $\sim$ 0.07 and 0.31 Å^2/ps for the BLYP (Ref. 62) and HCTH (Ref. 24) functionals. Diffusion constants of 0.07 ± 0.06 and 0.45 ± 0.20 Å^2/ps were calculated, respectively, for the nonreactive and reactive FM models developed here, where the value for the nonreactive model corresponds to solely vehicular transport (classical diffusion). The experimental value for the proton diffusion constant is 0.94 Å^2/ps.[63] These calculated values for the proton diffusion coefficients are considerably smaller than the experimental value, but this can be explained by the slower self-diffusion of the water combined with the fact that these are classical simulations and nuclear motion has not been quantized.[19] The self-diffusion of water for the current AIMD simulation is 0.04 ± 0.01 Å^2/ps, which is in agreement with a recently reported value using the same functional and dispersion correction.[39] The self-diffusion of water in the SPC/Fw water model used to develop the FM models for the excess proton is 0.23 ± 0.05 Å^2/ps, which agrees with the experimental value.[53,64]

C. Hydroxide ion

For the nonreactive FM hydroxide model, the inclusion of the three-body Stillinger-Weber potential leads to improved agreement with the AIMD results compared with results of the original two-site model.[21] The agreement with the current model in describing the hydroxide ion solvation structure, shown in Fig. 5, is similar to that of the charged-ring model, which was also force-matched to AIMD data,[21] as determined by comparison of the HH–OH–OW angle distributions. The corresponding reactive model also agrees with the AIMD results, such that the main peak in the full distribution is near 107°. There is still a noticeable contribution close to 180° in the reactive FM model, which largely arises from 4- and 5-coordinated species. The population of 5-coordinated species for the nonreactive model is larger than the AIMD result and the population is further enhanced in the reactive FM model with a corresponding decrease in the 3-coordinated species. The relative fraction of 4-coordinated species in the nonreactive and reactive FM models is nearly identical and $\sim$12% smaller than the AIMD result.

The RDFs for both the nonreactive and reactive hydroxide models are shown in Fig. 8. The same feature observed just beyond the first peak in the OH–OW RDF for the hydronium models can also be seen in the RDFs for the hydroxide models. Again, there is an enhanced peak between the two main peaks observed in the AIMD RDF, resulting from water

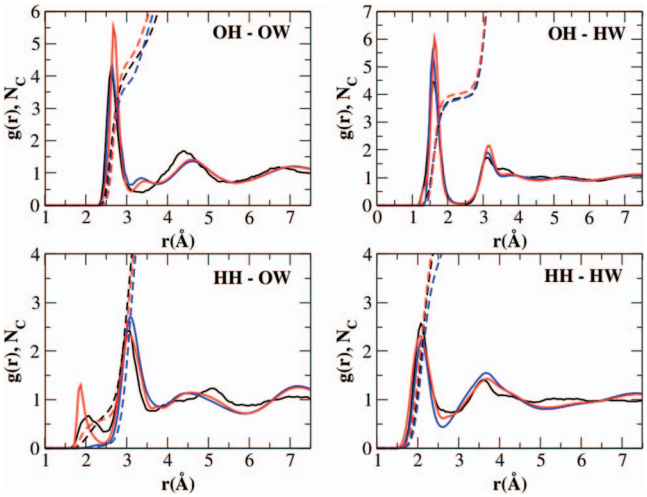

FIG. 8. Radial distribution functions (solid lines) and integrated coordination numbers (dashed lines) between atoms of the hydroxide ion and water molecules. For each plot, results from the AIMD (black), nonreactive (blue), and reactive MS-RMD (red) models are shown. The atom labels are defined in the text.

molecules being held too tightly. In this case, it is due to the water molecules that act as H-bond acceptors. The increased binding is consistent with increased peak heights and integrated coordination numbers for the two hydroxide-oxygen RDFs. Additional evidence for the increased binding of water molecules that accept an H-bond from the hydroxide ion can be seen in the HH–OW RDF and the narrowness of the first peak near 2.0 Å for the reactive model. The corresponding peak for water molecules that accept an H-bond from the hydroxide ion is not present in the nonreactive model, which is likely a result of the three-body HH–OH–OW potential acting on all nearby water molecules.

The free energy barrier for proton transfer between water and hydroxide is 1.6 and 1.9 kcal/mol for the AIMD and reactive models, respectively, as seen in Fig. 7. The self-diffusion of the hydroxide ion in the AIMD simulation was calculated to be 0.05 ± 0.02 Å^2/ps, which is larger than the calculated water self-diffusion constant, 0.02 ± 0.01 Å^2/ps, and smaller than that of the excess proton discussed above. This ordering of the diffusion constants is consistent with previous AIMD results and experiment.[65] The hydroxide diffusion constants calculated from the FM models are 0.08 ± 0.05 and 0.28 ± 0.20 Å^2/ps for the nonreactive and reactive models, respectively. The diffusion constant for the reactive MS-RDF model developed here is similar to the value calculated from a charged-ring MS-EVB model, 0.31 ± 0.03 Å^2/ps.[16]

IV. SUMMARY AND FUTURE OUTLOOK

In this work, a new force-matching-based reactive MD method was discussed with the goal of no longer relying on predefined empirical functions for the reactive models. With this iterative algorithm, numerical tabulated potentials can be used for all interactions including diabatic corrections and off-diagonal couplings in the MS-RMD framework. The flexibility and generality of the algorithm are illustrated by the development of reactive models for the excess proton and hydroxide in bulk water, which are nontrivial systems to model. The FM procedures used in this work are independent of the source of the reference data, thus enabling one to incorporate data from a number of configurational sampling methods and increasingly higher levels of theory. Using a general procedure to develop reactive models with a reduced number of constraints on the definition of the model, one can generate increasingly more accurate models that can reproduce the physical properties of the reference AIMD (or related) method, while at the same time extending the time and length scales accessible to the simulations at a significantly reduced computational cost.

ACKNOWLEDGMENTS

This research was supported in part by the National Science Foundation (NSF, Grant No. CHE-1214087) and the National Institutes of Health (NIH, Grant No. R01-GM053148). We also acknowledge support from the Department of Defense Multidisciplinary University Research Initiative through the (U.S.) Army Research Office (USARO Grant No. W911NF-10-1-0520), the (U.S.) Department of Energy (DOE) under Contract No. DE-AC02-06CH11357, and an Argonne National Laboratory (ANL) Computational Science Postdoctoral Fellowship to C.K. The computations in this work were supported in part by a grant of computer time from the U.S. Department of Defense (DOD) High Performance Computing Modernization Program at the Navy, Engineer Research and Development Center (ERDC), and Air Force Research Laboratory (AFRL) DOD Supercomputing Resource Centers. These computations were also supported in part by the National Science Foundation Teragrid and Extreme Science and Engineering Discovery Environment (XSEDE) computing resources provided by the Texas Advanced Computing Center under Grant No. MCA94P017.

[1] J. VandeVondele, M. Krack, F. Mohamed, M. Parrinello, T. Chassaing, and J. Hutter, Comput. Phys. Commun. **167**, 103 (2005).
[2] D. Marx and J. Hutter, *Ab Initio Molecular Dynamics: Basic Theory and Advanced Methods* (Cambridge University Press, Cambridge, New York, 2009).
[3] M. Guidon, J. Hutter, and J. VandeVondele, J. Chem. Theory Comput. **6**, 2348 (2010).
[4] B. Kirchner, P. J. d. Dio, and J. Hutter, Top. Curr. Chem. **307**, 109 (2012).
[5] C. Pisani, M. Schütz, S. Casassa, D. Usvyat, L. Maschio, M. Lorenz, and A. Erba, Phys. Chem. Chem. Phys. **14**, 7615 (2012).
[6] G. A. Voth, Acc. Chem. Res. **39**, 143 (2006).
[7] J. M. J. Swanson, C. M. Maupin, H. Chen, M. K. Petersen, J. Xu, Y. Wu, and G. A. Voth, J. Phys. Chem. B **111**, 4300 (2007).
[8] C. Knight and G. A. Voth, Acc. Chem. Res. **45**, 101 (2012).
[9] M. Ben-Nun, J. Quenneville, and T. J. Martínez, J. Phys. Chem. A **104**, 5161 (2000).
[10] N. L. Doltsinis and D. Marx, Phys. Rev. Lett. **88**, 166402 (2002).
[11] R. Mitrić, V. Bonačić-Koutecký, J. Pittner, and H. Lischka, J. Chem. Phys. **125**, 024303 (2006).
[12] I. Tavernelli, E. Tapavicza, and U. Rothlisberger, J. Mol. Struct.: -THEOCHEM **914**, 22 (2009).
[13] J. D. Watts, J. Gauss, and R. J. Bartlett, J. Chem. Phys. **98**, 8718 (1993).
[14] D. Borgis, G. Tarjus, and H. Azzouz, J. Chem. Phys. **97**, 1390 (1992).
[15] C. D. Wick and L. X. Dang, J. Phys. Chem. A **113**, 6356 (2009).
[16] I. S. Ufimtsev, A. G. Kalinichev, T. J. Martinez, and R. J. Kirkpatrick, Phys. Chem. Chem. Phys. **11**, 9420 (2009).
[17] G. Brancato and M. E. Tuckerman, J. Chem. Phys. **122**, 224507 (2005).
[18] C. D. Wick, J. Phys. Chem. C **116**, 4026 (2012).

[19]Y. Wu, H. Chen, F. Wang, F. Paesani, and G. A. Voth, J. Phys. Chem. B **112**, 7146 (2008).
[20]I. S. Ufimtsev, A. G. Kalinichev, T. J. Martinez, and R. J. Kirkpatrick, Chem. Phys. Lett. **442**, 128 (2007).
[21]C. Knight and G. A. Voth, Mol. Phys. **110**, 935 (2012).
[22]A. E. Lefohn, M. Ovchinnikov, and G. A. Voth, J. Phys. Chem. B **105**, 6628 (2001).
[23]E. Guàrdia and I. Skarmoutsos, J. Chem. Theory. Comput. **5**, 1449 (2009).
[24]C. Knight, C. M. Maupin, S. Izvekov, and G. A. Voth, J. Chem. Theory Comput. **6**, 3223 (2010).
[25]S. Izvekov and G. A. Voth, J. Phys. Chem. B **109**, 2469 (2005).
[26]S. Izvekov and G. A. Voth, J. Chem. Phys. **123**, 134105 (2005).
[27]W. G. Noid, J.-W. Chu, G. S. Ayton, and G. A. Voth, J. Phys. Chem. B **111**, 4116 (2007).
[28]W. G. Noid, J.-W. Chu, G. S. Ayton, V. Krishna, S. Izvekov, G. A. Voth, A. Das, and H. C. Andersen, J. Chem. Phys. **128**, 244114 (2008).
[29]W. G. Noid, P. Liu, Y. Wang, J.-W. Chu, G. S. Ayton, S. Izvekov, H. C. Andersen, and G. A. Voth, J. Chem. Phys. **128**, 244115 (2008).
[30]S. Izvekov and G. A. Voth, J. Phys. Chem. B **113**, 4443 (2009).
[31]L. Lu and G. A. Voth, J. Phys. Chem. B **113**, 1501 (2009).
[32]A. D. Becke, Phys. Rev. A **38**, 3098 (1988).
[33]C. Lee, W. Yang, and R. G. Parr, Phys. Rev. B **37**, 785 (1988).
[34]S. Grimme, J. Comput. Chem. **27**, 1787 (2006).
[35]J. Schmidt, J. VandeVondele, I.-F. W. Kuo, D. Sebastiani, J. I. Siepmann, J. Hutter, and C. J. Mundy, J. Phys. Chem. B **113**, 11959 (2009).
[36]I.-C. Lin, A. P. Seitsonen, M. D. Coutinho-Neto, I. Tavernelli, and U. Rothlisberger, J. Phys. Chem. B **113**, 1127 (2009).
[37]J. Wang, G. Román-Pérez, J. M. Soler, E. Artacho, and M.-V. Fernández-Serra, J. Chem. Phys. **134**, 024516 (2011).
[38]S. Yoo and S. S. Xantheas, J. Chem. Phys. **132**, 121105 (2011).
[39]M. D. Baer, C. J. Mundy, M. J. McGrath, I.-F. W. Kuo, J. I. Siepmann, and D. J. Tobias, J. Chem. Phys. **135**, 124712 (2011).
[40]J. VandeVondele and J. Hutter, J. Chem. Phys. **118**, 4365 (2003).
[41]S. Goedecker, M. Teter, and J. Hutter, Phys. Rev. B **54**, 1703 (1996).
[42]U. W. Schmitt and G. A. Voth, J. Phys. Chem. B **102**, 5547 (1998).
[43]A. Warshel and R. M. Weiss, J. Am. Chem. Soc. **102**, 6218 (1980).
[44]A. Warshel, *Computer Modeling of Chemical Reactions in Enzymes and Solutions* (Wiley, New York, NY, 1991).
[45]J. Åqvist and A. Warshel, Chem. Rev. **93**, 2523 (1993).
[46]A. Warshel, Annu. Rev. Biophys. Biomol. Struct. **32**, 425 (2003).
[47]U. W. Schmitt and G. A. Voth, J. Chem. Phys. **111**, 9361 (1999).
[48]T. J. F. Day, A. V. Soudackov, M. Čuma, U. W. Schmitt, and G. A. Voth, J. Chem. Phys. **117**, 5839 (2002).
[49]Y. Kim, J. C. Corchado, J. Villà, J. Xing, and D. G. Truhlar, J. Chem. Phys. **112**, 2718 (2000).
[50]M. Higashi and D. G. Truhlar, J. Chem. Theory Comput. **5**, 2925 (2009).
[51]K. F. Wong, J. L. Sonnenberg, F. Paesani, T. Yamamoto, J. Vanicek, W. Zhang, H. B. Schlegel, D. A. Case, T. E. Cheatham III, W. H. Miller, and G. A. Voth, J. Chem. Theory Comput. **6**, 2566 (2010).
[52]M. A. Bellucci and D. F. Coker, J. Chem. Phys. **135**, 044115 (2011).
[53]Y. Wu, H. L. Tepper, and G. A. Voth, J. Chem. Phys. **124**, 024503 (2006).
[54]J. M. J. Swanson and J. Simons, J. Phys. Chem. B **113**, 5149 (2009).
[55]O. Markovitch, H. Chen, S. Izvekov, F. Paesani, G. A. Voth, and N. Agmon, J. Phys. Chem. B **112**, 9456 (2008).
[56]S. Izvekov, M. Parrinello, C. J. Burnham, and G. A. Voth, J. Chem. Phys. **120**, 10896 (2004).
[57]S. Izvekov and G. A. Voth, J. Phys. Chem. B **109**, 6573 (2005).
[58]L. Lu, S. Izvekov, A. Das, H. C. Andersen, and G. A. Voth, J. Chem. Theory Comput. **6**, 954 (2010).
[59]F. H. Stillinger and T. A. Weber, Phys. Rev. B **31**, 5262 (1985).
[60]S. J. Plimpton, J. Comp. Phys. **117**, 1 (1995).
[61]D. Marx, M. E. Tuckerman, J. Hütter, and M. Parrinello, Nature (London) **397**, 601 (1999).
[62]S. Izvekov and G. A. Voth, J. Chem. Phys. **123**, 044505 (2005).
[63]N. K. Roberts and H. L. Northey, J. Chem. Soc., Faraday Trans. 1 **70**, 253 (1974).
[64]K. Krynicki, C. D. Green, and D. W. Sawyer, Faraday Discuss. Chem. Soc. **66**, 199 (1978).
[65]D. Marx, A. Chandra, and M. E. Tuckerman, Chem. Rev. **110**, 2174 (2010).